Eliashberg Theory for Dynamical Screening in Bilayer Exciton Condensation

G. J. Sreejith,[1,2] Jay D. Sau,[2] and Sankar Das Sarma[2]
[1]Indian Institute of Science Education and Research, Pune 411008, India
[2]Condensed Matter Theory Center and Joint Quantum Institute, Department of Physics, University of Maryland, College Park, Maryland 20742–4111, USA

(Received 14 February 2024; revised 14 May 2024; accepted 25 June 2024; published 29 July 2024)

We study the effect of dynamical screening of interactions on the transition temperatures (T_c) of exciton condensation in a symmetric bilayer of quadratically dispersing electrons and holes by solving the linearized Eliashberg equations for the anomalous interlayer Green's functions. We find that T_c is finite for the range of density and layer separations studied, decaying exponentially with interlayer separation. T_c is suppressed well below that predicted by a Hartree Fock mean field theory with unscreened Coulomb interaction, but is above the estimates from the statically screened Coulomb interaction. Furthermore, using a diagrammatic framework, we show that the system is always an exciton condensate at zero temperature but T_c is exponentially small for large interlayer separation.

DOI: 10.1103/PhysRevLett.133.056501

The possibility of Bose-Einstein condensation (BEC) of interlayer excitons formed due to the attractive interaction between electrons and holes in oppositely doped semiconductor bilayers [1–5] has been studied extensively over the past six decades, however, experimental evidence in semiconductor systems outside the quantum Hall regime [6] has been absent. Recent advances in precision control of particle-hole symmetric electron-hole bilayers have brought us closer to their realization [7–14] making conceptual questions of their phase diagram of current relevance.

In addition to the condensate phase, the electron hole bilayer system could exhibit a rich phase diagram containing supersolid, density wave, Wigner crystal, FFLO, and Fermi liquid phases as the temperature, interlayer separation (d), electron density, screening, interlayer tunneling, and layer imbalance are tuned [15–17]. However, the precise zero temperature phase diagram of the symmetric bilayer is not yet settled. Different calculational approaches agree when d is less than the intralayer particle separation —electrons and holes pair up across the layers to form excitons that undergo a BEC below some finite temperature T_c. The attractive interaction weakens rapidly with d and there are two possible scenarios in the opposite limit of large d—(a) an exciton condensate is always formed albeit at a vanishingly small T_c or (b) the exciton condensate is very unstable and forms an electron-hole plasma even at zero temperature (potentially due to intralayer screening). Mean field calculations employing different static-screening approximations produce different results. Unscreened [18,19] as well as static-screening approximations based on normal state correlations show a zero-temperature excitonic condensate phase [20,21] whereas approximations that incorporate condensatelike correlations in the screening suggest a critical separation beyond which the condensate is absent. Variational and diffusion Monte Carlo studies using ansatz wave functions also indicate an electron-hole plasma [20,22–25]. Similar results are also obtained in graphenelike linear dispersion systems at large d (or large carrier density) [26–28].

In the present work, we go beyond the simple Hartree-Fock and static-screening approximations and quantitatively investigate the effect of dynamical screening using the dynamical random phase approximation (RPA) on the T_c by solving the Eliashberg equations [29,30] for the anomalous interlayer Green's functions taking into account the corrected quasiparticle residue, while restricting to the screening calculated from the normal state polarization. Since Eliashberg theory is the most complete theory for calculating T_c in superconductors, with great success in predicting quantitatively accurate T_c [31], for many superconducting materials, our Letter is of great significance in understanding electron-hole condensation in 2D bilayer structures. In addition, we show that the diagrams contained in the Eliashberg framework can be extended in the Fermi liquid regime to show that the excitonic instability is robust for arbitrarily weak interlayer interactions.

Our model consists of electrons (represented by ψ_1 of charge $-e$) in one layer ($l = 1$) and holes (ψ_2 of charge e) in the other layer ($l = 2$), separated by a distance d. In order to address the question of the symmetric bilayer with no interlayer tunneling, we assume identical quadratic dispersions and chemical potentials in the two layers and ignore spin degrees of freedom (changing dispersion does not modify any of our qualitative conclusions). The carriers interact via the attractive (repulsive) Coulomb coupling in the interlayer (intralayer) channel. The Hamiltonian for the system is given by

$$H = H_0 + H_{\text{intra}} + H_{\text{inter}} \tag{1}$$

where

$$H_0 = \sum_{l=1,2} \int_k (\varepsilon_k - \mu) \psi^\dagger_{l,\vec{k}} \psi_{l,\vec{k}} \tag{2}$$

where the dispersion is given by $\varepsilon_k = (\hbar^2 k^2/2m)$, $\mu = \varepsilon_{K_F}$ is the bare Fermi energy, K_F is the Fermi wave vector and $\int_{k_1,k_2,\ldots}$ represents $\prod_{i=1,\ldots} d^2k_i/(2\pi)^2$.

The intralayer and interlayer interaction Hamiltonians are

$$H_{\text{intra}} = \frac{1}{2} \sum_{l=1,2} \int_{k,p,q} V_q \psi^\dagger_{l,\vec{k}+\vec{q}} \psi^\dagger_{l,\vec{p}-\vec{q}} \psi_{l,\vec{p}} \psi_{l,\vec{k}},$$
$$H_{\text{inter}} = -\int_{k,p,q} U_q \psi^\dagger_{1,\vec{k}+\vec{q}} \psi^\dagger_{2,\vec{p}-\vec{q}} \psi_{2,\vec{p}} \psi_{1,\vec{k}}. \tag{3}$$

The bare intralayer repulsion ($V_q > 0$) and interlayer attraction ($U_q > 0$) are

$$V_q = \frac{e^2}{2\epsilon} \frac{1}{q}, \qquad U_q = \frac{e^2}{2\epsilon} \frac{e^{-qd}}{q}, \tag{4}$$

where ϵ is the average dielectric constant. We assume that both layers have background lattices of neutralizing charges (e.g., gates) that cancel the Hartree terms.

A simple fermion renormalization group (RG) analysis [32] at one loop suggests an exciton pairing instability at any d because of the Copper pairing induced by the interlayer electron-hole attraction which cannot be made repulsive by any amount of screening. Starting from the Fermi liquid fixed points of the intralayer Hamiltonians, the effective attractive coupling $U_{\text{qp}} > 0$ between the quasiparticles of the layers at the wave vector $2K_F$ evolves under RG at one loop as

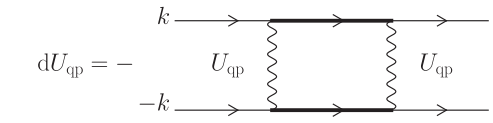

where the thick lines indicate integration over a thin momentum shell of energy between E and $E + \mathrm{d}E$ above and below the Fermi surface. For any attractive bare coupling between the quasiparticles of the Fermi liquid $u > 0$, U_{qp} diverges as $U_{\text{qp}} \sim (1 - u \ln E/8\pi)^{-1}$. We expect this description to remain valid in the limit of large d where the weak interlayer interactions may not affect the initial RG flow from the microscopic intralayer Hamiltonian to the vicinity of the Fermi liquid fixed points. Consequentially, we expect the exciton instability to survive at large d as long as u is negative. This expectation can be validated by a more rigorous diagrammatic analysis whose details are presented in Supplemental Material (SM) [33], which shows that the RG expectation is valid at lowest order in interlayer interaction U and to all orders in intralayer interactions provided the Fermi liquid Green function survives. The only difference is that the parameter u is related to the bare interlayer interaction U through some vertex corrections. The current work carries out a careful quantitative estimate of the effect of the dynamical screening to calculate the transition temperatures and establishes that the expectation from RG holds true, even when dynamical screening effects are included.

Within RPA the dynamically screened interlayer and intralayer interactions are given by

$$U^{\text{eff}}_{\boldsymbol{q}} = \sum$$ 

$$V^{\text{eff}}_{\boldsymbol{q}} = \sum$$ 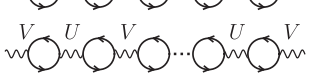

where the sums are over the number of polarization bubbles (Π) and also the possible types (U or V) of interaction lines between them such that summands of $V^{\text{eff}}_{\boldsymbol{q}}$ and $U^{\text{eff}}_{\boldsymbol{q}}$ contain even and odd numbers of bare U_q interaction lines respectively. Because of the symmetry of the layers, Π is independent of the layer index. The dynamically screened interactions are given by

$$V^{\text{eff}}_{\boldsymbol{q}} = \frac{1}{2} \sum_{\sigma=\pm 1} \frac{V_q + \sigma U_q}{1 + (V_q + \sigma U_q)\Pi_{\boldsymbol{q}}},$$
$$U^{\text{eff}}_{\boldsymbol{q}} = \frac{1}{2} \sum_{\sigma=\pm 1} \sigma \frac{V_q + \sigma U_q}{1 + (V_q + \sigma U_q)\Pi_{\boldsymbol{q}}}. \tag{5}$$

We use $\vec{p}$ for 2D wave vectors, p for their magnitudes and bold font $\boldsymbol{p}$ for the tuple $(\vec{p}, \imath\omega_p)$ where ω_p is the Matsubara frequency. The bare polarization function at low temperature is given by (SM [33]):

$$\Pi_{\boldsymbol{q}} = \frac{m}{2\pi\hbar^2} \left[1 - \text{Re} \sqrt{\left(1 - \imath \frac{\hbar\omega_q}{q^2\hbar^2/2m}\right)^2 - \frac{K_F^2}{q^2/4}} \right], \tag{6}$$

which is the analytic continuation in the upper-half of the complex ω plane of real-frequency polarization function given in [35].

We define the normal ($\mathcal{G}$) and anomalous ($\mathcal{F}$) imaginary time Green's functions, in the usual manner, as

$$\mathcal{G}(\vec{p}, \tau) = -\langle T_\tau \psi_{l,\vec{p}}(\tau) \psi^\dagger_{l,\vec{p}}(0) \rangle,$$
$$\mathcal{F}(\vec{p}, \tau) = -\langle T_\tau \psi_{1,-\vec{p}}(\tau) \psi_{2,\vec{p}}(0) \rangle. \tag{7}$$

The symmetry between the two layers makes the normal Green's function identical in the layers. The normal Matsubara Green's function satisfies the following Dyson equation

$$\frac{\mathcal{G}_p}{\mathcal{G}_p^0} = 1 + \frac{1}{\hbar}\Sigma_p \mathcal{G}_p - \frac{1}{\hbar} W_p F_p^\dagger, \tag{8}$$

with the normal and anomalous self-energies (Σ and W, respectively)

$$\Sigma_q = \frac{-1}{\hbar\beta}\sum_{\iota\omega_k}\int_k V^{\rm eff}_{q-k}\mathcal{G}_k, \quad W_q = \frac{1}{\hbar\beta}\sum_{\iota\omega_k}\int_k U^{\rm eff}_{q-k}\mathcal{F}_k, \tag{9}$$

$\beta = 1/k_B T$, and $\mathcal{G}_k$, $\mathcal{F}_k$ represent the Matsubara space functions obtained by suitable Fourier transforms of the imaginary time functions $\mathcal{G}(\vec{k},\tau)$, $\mathcal{F}(\vec{k},\tau)$. The exciton condensation is defined by a nonzero anomalous self-energy which is related to the condensate order parameter as $\Delta_q \sim W_q/Z_q$.

Using the Dyson equation, these can be expressed as a set of coupled Eliashberg equations incorporating dynamical screening in the exciton condensate formation. It is convenient to express the normal self-energy in terms of parts that are even and odd in frequency, parametrized by S and Z, respectively, as $\Sigma_q = S_q + \iota\omega_q(1 - Z_q)$. The Eliashberg equations can then be expressed as

$$\begin{aligned} Z_q &= 1 - \frac{1}{\hbar\beta}\sum_{\iota\omega_k}\int_k V^{\rm eff}_{q-k}\frac{\iota\omega_k}{\iota\omega_q}\frac{Z_k}{\Lambda_k}, \\ S_q &= \frac{1}{\hbar\beta}\sum_{\iota\omega_k}\int_k V^{\rm eff}_{q-k}\frac{\frac{1}{\hbar}E_k}{\Lambda_k}, \\ W_q &= \frac{1}{\hbar\beta}\sum_{\iota\omega_k}\int_k U^{\rm eff}_{q-k}\frac{W_k}{\Lambda_k}, \end{aligned} \tag{10}$$

where $\Lambda_k = [\omega_k Z_k]^2 + (1/\hbar^2)(E_k^2 + W_k^2)$ and $E_k = \epsilon_k + S_k - \mu$.

The anomalous self-energy W_q is zero at high temperatures and becomes finite as the temperature is lowered if there is a transition into an excitonic condensate phase. We estimate the transition temperature T_c by numerically solving a linearized (in W) form of the above equations which is valid near T_c. We assume full rotational invariance and consider only s-wave solutions, as a result of which W, S, and Z depend only on $(q, \iota\omega_q)$.

Static screening—Before considering the solution to the Eliashberg equations, we consider a static screening approximation—we ignore corrections to Z, setting it to the bare value 1, and ignore frequency dependences of S, W, $V^{\rm eff}$, and $U^{\rm eff}$. After performing the Matsubara summations in Eq. (10), we get the following mean field equations

$$\begin{aligned} \Sigma_q &= \frac{1}{2}\int_q V_q^0\left[\frac{E_q}{\xi_q}\tanh\frac{\beta\xi_q}{2} - 1\right], \\ W_q &= \frac{1}{2}\int_q U_q^0\left[\frac{E_q}{\xi_q}\tanh\frac{\beta\xi_q}{2}\right], \end{aligned} \tag{11}$$

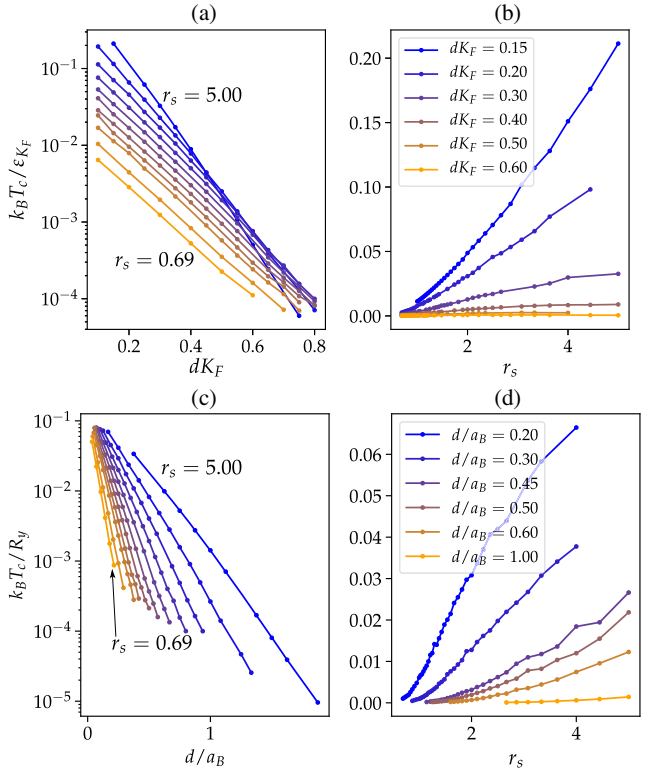

FIG. 1. T_c from the screened HF mean field equations (a) T_c/T_F as a function of the dimensionless interlayer separation dK_F for different values of r_s. T_c decreases rapidly but remains finite even for the largest values of d. (b) T_c/T_F for fixed values of dK_F increases with r_s except at very large r_s and dK_F. (c),(d) Similar to (a),(b) but in atomic units.

where $E_q = \varepsilon_q + \Sigma_q - \mu$ and $\xi = (E_q^2 + W_q^2)^{1/2}$. The statically screened interactions V_q^0 and U_q^0 are the zero frequency limits of the effective interactions shown in Eq. (5). Figure 1 shows the transition temperatures obtained by solving the equations numerically, presented as a function of the Wigner Seitz interaction radius $r_s = 2/a_{\rm B}K_F$ (i.e., the dimensionless intralayer particle separation), where $a_{\rm B}$ is the Bohr radius. We find that the transition temperatures T_c in Fermi units (Fermi temperature $T_F = \varepsilon_{K_F}/k_B$ and $1/K_F$ as units of temperature and length, respectively) decays exponentially as a function of d.

Equations (11) are the Hartree-Fock (HF) mean field equations analyzed in Refs. [18,19,36], except for the use of unscreened interactions. An unscreened approximation can be obtained by replacing the interactions V^0 and U^0 with the bare Coulomb interactions [Eq. (4)]. Figure 2 shows the T_c obtained by solving the unscreened mean field equations. Panel (a) shows T_c/T_F as a function of dK_F. Panel (c) shows the similar data but with the T_c and d in atomic units ($R_y/k_B = (1/k_B)(e^2/8\pi\epsilon a_B)$ and a_B as units for temperature and length).

In both static approximations (unscreened and statically screened HF), we find that T_c decays rapidly with increasing d approximately exponentially when plotted in Fermi

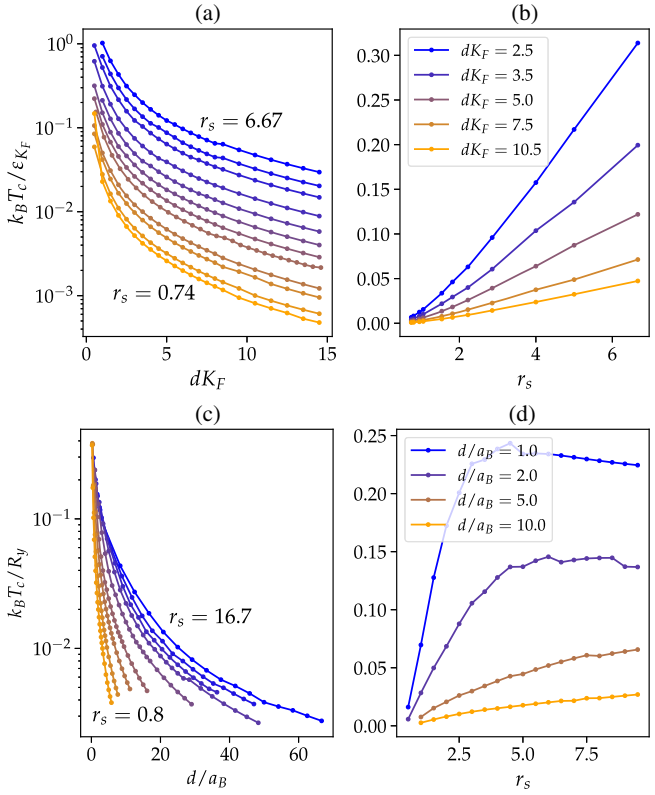

FIG. 2. T_c from the unscreened HF mean field equations. (a) T_c/T_F as a function of dK_F for different values of r_s. (b) T_c/T_F for fixed separations dK_F increases with r_s. (c),(d) Similar to (a),(b) but with axes in atomic units.

units. The statically screened mean field equations predict a very small T_c which is consistent with previous observations in multicomponent systems [21,37]. The T_c increases with r_s but tends to saturate at very large r_s [19].

Dynamical screening—To obtain T_c we numerically estimate the magnitude of the eigenvalue that governs the evolution of $W_{\boldsymbol{q}}$ under iterations of the linearized self-consistent Eliashberg equations treated as a recursive relation. The eigenvalue decreases with T and is 1 at T_c. The linearized (in W) equations for S and Z are independent of W and can be solved first using iterations, these are found to converge rapidly [38] and these results can be used in the equations for W whose leading eigenvalue can be determined by power iteration method.

Following Ref. [39], we find it convenient to decompose the even part of the self-energy S into frequency dependent and independent components:

$$S_{\boldsymbol{q}} = S^{\omega}_{\boldsymbol{q}} + S^{0}_{q} \tag{12}$$

where the frequency dependent component

$$S^{\omega}_{\boldsymbol{q}} = \frac{1}{\hbar\beta}\sum_{\imath\omega_k}\int_k (V^{\mathrm{eff}}_{\boldsymbol{k}-\boldsymbol{q}} - V_{|\vec{k}-\vec{q}|})\frac{E_{\boldsymbol{k}}/\hbar}{\Lambda_{\boldsymbol{k}}} \tag{13}$$

is found to vanish at large wave vectors and frequencies [39] and therefore has a finite support in the q-ω plane (the cutoffs for this are set at $q = 40K_F$ and $\hbar\omega \sim 50\varepsilon_{K_F}$ in the numerics). Same cutoffs are used for $Z_{\boldsymbol{q}}$ which asymptotes to 1 at large frequencies and wave vectors. Matsubara sums are performed, in all cases at least up to $\hbar\omega_k = 135\varepsilon_{K_F}$ even at low temperatures.

The frequency independent component of S can be written as

$$S^{0}_{q} = \frac{1}{\hbar\beta}\int_k V_{|\vec{k}-\vec{q}|}\sum_{\imath\omega_k}\left(\frac{E_{\boldsymbol{k}}/\hbar}{\Lambda_{\boldsymbol{k}}} - \frac{1}{2}\right). \tag{14}$$

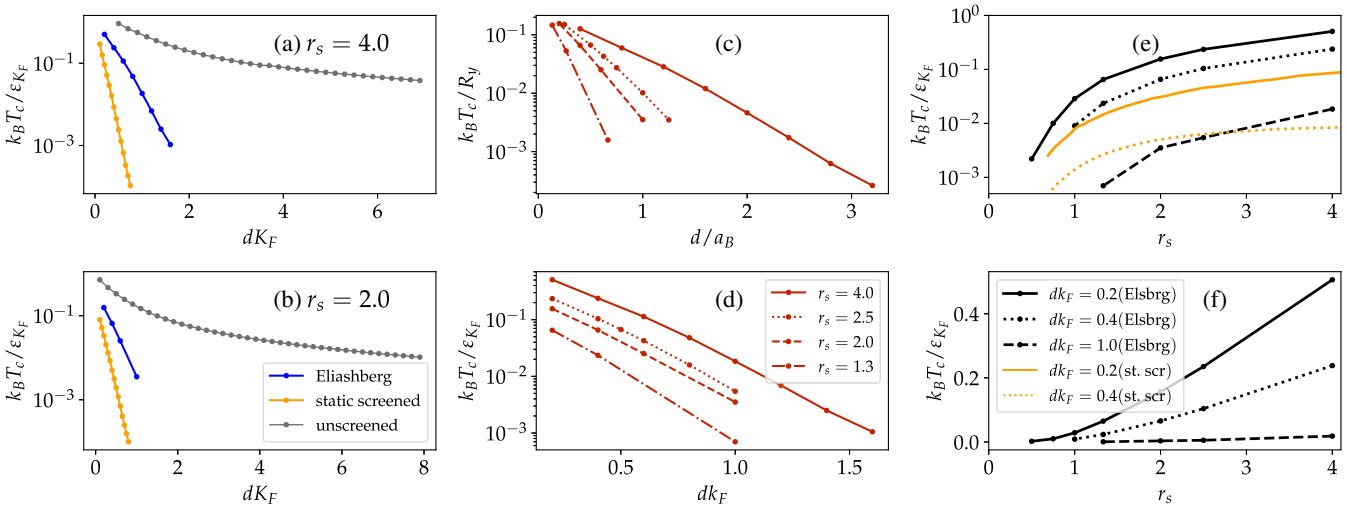

FIG. 3. T_c estimates from Eliashberg equations (a),(b) Comparison of the T_c estimated from the Eliashberg equations (blue) and the static screening approximations. (c),(d) T_c for different r_s as a function of d plotted in Fermi and atomic units. (e),(f) T_c as a function of r_s for fixed values of d. Orange lines in (e) show the results for the statically screened approximations for the corresponding values of d and r_s. Plots in a column share the same legend.

The chemical potential μ is tuned self-consistently to satisfy $E_{K_F}(\omega = 0) = 0$ keeping the Fermi wave vector fixed. S^0 can be efficiently estimated to high accuracy (see SM [33]). The gap $W_{\boldsymbol{q}}$ vanishes at large wave vector and saturates to a q-dependent constant W_q^∞ at large frequency, for which we set a cutoff (to reach saturation) of $\hbar\omega \sim 50\varepsilon_{K_F}$. Representative plots of S, W, and Z are shown in Supplemental Material [33].

Figure 3 shows the T_c estimated from solving the Eliashberg equations. T_c/T_F decreases exponentially but remains finite for all r_s and d. Dynamical screening suppresses the T_c/T_F to a value smaller than the estimates from unscreened approximations. Approximate treatment of dynamical screening effects [40] in graphene have indicated a first order transition as a function of distance. Within the range of distances where we could reliably perform our calculations we do not find such a transition. T_c at fixed r_s exponentially decays with d till the largest value that we could study. At fixed d, and decreasing r_s, T_c again remains finite up to the smallest r_s we could access.

Eliashberg theory is known to be insufficient when the frequency scales of the attractive interaction (along the real-frequency axis) are comparable to the Fermi energy [29]. In our case the dominant frequency content of U^{eff} correspond to the plasmons of the 2D system which have small frequencies on account of its $\hbar\omega/E_F \sim \sqrt{r_s q}$ dispersion. This is especially true at small r_s and large d where the plasmon mode diffuses into the particle-hole continuum as the frequency is increased (see SM [33] where we show the spectral function of U^{eff} averaged over the Fermi surface).

Our main findings are (1) T_c is finite always, but exponentially small for large d; (2) T_c is lower than that obtained from the unscreened HF theory; (3) interlayer coherent exciton condensate exists for all parameters at $T = 0$. The reason for the bilayer to be always interlayer coherent at $T = 0$ is that the interlayer interaction is always attractive, and this implies that there is no repulsion-induced μ^* effect in T_c as in metallic superconductors [41]—all that intralayer interactions can do is to suppress the effective interlayer attraction, but can never make it vanish, implying that T_c is always finite albeit very small for large d. This expectation is argued to be correct beyond Eliashberg theory (i.e., including arbitrary intralayer vertex corrections) where a bound on T_c that is comparable to the static screening limit is obtained for the general Bethe-Salpeter equation.

Acknowledgments—G. J. S. thanks Yang-Zhi Chou, Andrey Grankin, Darshan Joshi, R. Sensarma, A. Balatsky, and F Marsiglio for useful inputs. This work is supported by the Laboratory for Physical Sciences. One of the authors (G. J. S) acknowledges partial JQI support for a sabbatical leave. The authors also thank National Supercomputing Mission (NSM), India for providing the computing resources of "PARAM Brahma" at IISER Pune, which is implemented by C-DAC and supported by the Ministry of Electronics and Information Technology (MeitY) and Department of Science and Technology (DST), Government of India.

[1] L. Keldysh and Y. V. Kopaev, Possible instability of the semimetallic state toward Coulomb interaction, Fiz. Tverd. Tela **6**, 2791 (1964).
[2] J. D. Cloizeaux, Exciton instability and crystallographic anomalies in semiconductors, J. Phys. Chem. Solids **26**, 259 (1965).
[3] D. Jérome, T. M. Rice, and W. Kohn, Excitonic insulator, Phys. Rev. **158**, 462 (1967).
[4] Y. E. Lozovik and V. I. Yudson, Feasibility of superfluidity of paired spatially separated electrons and holes; A new superconductivity mechanism, JETP Lett. **22**,11 (1975).
[5] C. Comte and P. Nozières, Exciton Bose condensation: The ground state of an electron-hole gas—I. Mean field description of a simplified model, J. Phys. **43**, 1069 (1982).
[6] J. Eisenstein, Exciton condensation in bilayer quantum Hall systems, Annu. Rev. Condens. Matter Phys. **5**, 159 (2014).
[7] J. I. A. Li, T. Taniguchi, K. Watanabe, J. Hone, and C. R. Dean, Excitonic superfluid phase in double bilayer graphene, Nat. Phys. **13**, 751 (2017).
[8] Z. Wang, D. A. Rhodes, K. Watanabe, T. Taniguchi, J. C. Hone, J. Shan, and K. F. Mak, Evidence of high-temperature exciton condensation in two-dimensional atomic double layers, Nature (London) **574**, 76 (2019).
[9] L. Ma, P. X. Nguyen, Z. Wang, Y. Zeng, K. Watanabe, T. Taniguchi, A. H. MacDonald, K. F. Mak, and J. Shan, Strongly correlated excitonic insulator in atomic double layers, Nature (London) **598**, 585 (2021).
[10] D. Chen, Z. Lian, X. Huang, Y. Su, M. Rashetnia, L. Ma, L. Yan, M. Blei, L. Xiang, T. Taniguchi *et al.*, Excitonic insulator in a heterojunction moiré superlattice, Nat. Phys. **18**, 1171 (2022).
[11] B. Sun, W. Zhao, T. Palomaki, Z. Fei, E. Runburg, P. Malinowski, X. Huang, J. Cenker, Y.-T. Cui, J.-H. Chu *et al.*, Evidence for equilibrium exciton condensation in monolayer WTe2, Nat. Phys. **18**, 94 (2022).
[12] Z. Zhang, E. C. Regan, D. Wang, W. Zhao, S. Wang, M. Sayyad, K. Yumigeta, K. Watanabe, T. Taniguchi, S. Tongay *et al.*, Correlated interlayer exciton insulator in heterostructures of monolayer WSe_2 and moiré WS_2/WSe_2, Nat. Phys. **18**, 1214 (2022).
[13] Z. Lei, E. Cheah, F. Krizek, R. Schott, T. Bähler, P. Märki, W. Wegscheider, M. Shayegan, T. Ihn, and K. Ensslin, Gate-defined two-dimensional hole and electron systems in an undoped InSb quantum well, Phys. Rev. Res. **5**, 013117 (2023).
[14] M. L. Davis, S. Parolo, C. Reichl, W. Dietsche, and W. Wegscheider, Josephson-like tunnel resonance and large Coulomb drag in GaAs-based electron-hole bilayers, Phys. Rev. Lett. **131**, 156301 (2023).
[15] Y. N. Joglekar, A. V. Balatsky, and S. Das Sarma, Wigner supersolid of excitons in electron-hole bilayers, Phys. Rev. B **74**, 233302 (2006).

[16] J.-X. Zhu and A. R. Bishop, Exciton condensate modulation in electron-hole bilayers: A real-space visualization, Phys. Rev. B **81**, 115329 (2010).
[17] M. M. Parish, F. M. Marchetti, and P. B. Littlewood, Supersolidity in electron-hole bilayers with a large density imbalance, Europhys. Lett. **95**, 27007 (2011).
[18] P. B. Littlewood and X. Zhu, Possibilities for exciton condensation in semiconductor quantum-well structures, Phys. Scr. T **68**, 56 (1996).
[19] X. Zhu, P. B. Littlewood, M. S. Hybertsen, and T. M. Rice, Exciton condensate in semiconductor quantum well structures, Phys. Rev. Lett. **74**, 1633 (1995).
[20] D. Neilson, A. Perali, and A. R. Hamilton, Excitonic superfluidity and screening in electron-hole bilayer systems, Phys. Rev. B **89**, 060502(R) (2014).
[21] M. Y. Kharitonov and K. B. Efetov, Electron screening and excitonic condensation in double-layer graphene systems, Phys. Rev. B **78**, 241401(R) (2008).
[22] S. De Palo, F. Rapisarda, and G. Senatore, Excitonic condensation in a symmetric electron-hole bilayer, Phys. Rev. Lett. **88**, 206401 (2002).
[23] R. Maezono, P. López Ríos, T. Ogawa, and R. J. Needs, Excitons and biexcitons in symmetric electron-hole bilayers, Phys. Rev. Lett. **110**, 216407 (2013).
[24] P. López Ríos, A. Perali, R. J. Needs, and D. Neilson, Evidence from quantum Monte Carlo simulations of large-gap superfluidity and BCS-BEC crossover in double electron-hole layers, Phys. Rev. Lett. **120**, 177701 (2018).
[25] S. Conti, A. Perali, A. R. Hamilton, M. V. Milošević, F. m. c. M. Peeters, and D. Neilson, Chester supersolid of spatially indirect excitons in double-layer semiconductor heterostructures, Phys. Rev. Lett. **130**, 057001 (2023).
[26] H. Min, R. Bistritzer, J.-J. Su, and A. H. MacDonald, Room-temperature superfluidity in graphene bilayers, Phys. Rev. B **78**, 121401(R) (2008).
[27] F. Nilsson and F. Aryasetiawan, Effects of dynamical screening on the BCS-BEC crossover in double bilayer graphene: Density functional theory for exciton bilayers, Phys. Rev. Mater. **5**, L050801 (2021).
[28] A. Perali, D. Neilson, and A. R. Hamilton, High-temperature superfluidity in double-bilayer graphene, Phys. Rev. Lett. **110**, 146803 (2013).
[29] F. Marsiglio, Eliashberg theory: A short review, Ann. Phys. (Amsterdam) **417**, 168102 (2020), Eliashberg theory at 60: Strong-coupling superconductivity and beyond.
[30] R. D. Parks, *Superconductivity*, 1st ed. (CRC Press, Boca Raton, 1969).
[31] A. V. Chubukov, A. Abanov, I. Esterlis, and S. A. Kivelson, Eliashberg theory of phonon-mediated superconductivity—When it is valid and how it breaks down, Ann. Phys. (Amsterdam) **417**, 168190 (2020).
[32] R. Shankar, Renormalization-group approach to interacting fermions, Rev. Mod. Phys. **66**, 129 (1994).
[33] See Supplemental Material at http://link.aps.org/supplemental/10.1103/PhysRevLett.133.056501, which discusses the polarization function, effective action approach and solutions to the Eliashberg equations, and which includes Ref. [34].
[34] G. Strinati, Application of the Green's functions method to the study of the optical properties of semiconductors, Riv. Nuovo Cimento **11**, 1 (1988).
[35] F. Stern, Polarizability of a two-dimensional electron gas, Phys. Rev. Lett. **18**, 546 (1967).
[36] J. Zhu and S. D. Sarma, Interaction and coherence in two-dimensional bilayers, Phys. Rev. B **109**, 085129 (2024).
[37] D. S. L. Abergel, R. Sensarma, and S. Das Sarma, Density fluctuation effects on the exciton condensate in double-layer graphene, Phys. Rev. B **86**, 161412(R) (2012).
[38] A. Grankin and V. Galitski, Interplay of hyperbolic plasmons and superconductivity, Phys. Rev. B **108**, 094506 (2023).
[39] H. Rietschel and L. J. Sham, Role of electron Coulomb interaction in superconductivity, Phys. Rev. B **28**, 5100 (1983).
[40] I. Sodemann, D. A. Pesin, and A. H. MacDonald, Interaction-enhanced coherence between two-dimensional Dirac layers, Phys. Rev. B **85**, 195136 (2012).
[41] P. B. Allen and R. C. Dynes, Transition temperature of strong-coupled superconductors reanalyzed, Phys. Rev. B **12**, 905 (1975).